Journal of the Korean Nuclear Society
Volume 31, Number 3, pp.276~286, June 1999

Analysis of the Relations Between Design Parameters and Performance in the Passive Safety Decay Heat Removal System

Sim Yoon Sub, Wi Myung Hwan, Kim Eui Kwang, and Min Beong Tae
Korea Atomic Energy Research Institute
150 Dukjin-dong, Yusong-gu, Taejon 305-353, Korea
yssim@nanum.kaeri.re.kr

(Received September 21, 1998)

Abstract

A computer code PARS2 is developed for the analysis of PSDRS, which is the safety grade RHRS of KALIMER, and applied to the investigation of the relation between design parameters and performance of PSDRS. The concept of the heat transfer resistance network is applied in assessing the importance of the various heat transfer modes. From the analysis results, the qualitative relations between the PSDRS performance and design parameters are found and guidelines for the PSDRS design procedures are also proposed.

Key Words : decay heat removal, PSDRS, radiation heat transfer, enhancement, KALIMER

1. Introduction

The PSDRS(Passive Safety Decay Heat Removal System) is the safety grade system that removes decay heat in KALIMER[1,2]. KALIMER is a liquid metal reactor under development at KAERI. Core decay heat is removed passively from the core to the plant environment air by the natural circulation. Its structure is shown in Fig.1. Since its operation is based on the natural passive mechanism, it is highly reliable and plant decay heat can be safely removed without external support during an accident. The decay heat from the core is transferred to the reactor vessel by the natural circulation of the sodium in the reactor pool and the heat is in turn transferred by conduction and radiation to the containment vessel. The hot containment vessel wall heats the surrounding air in the air channel and the density difference between the air inside and that outside the channel induces the pressure difference. This difference forms air flow and the heat is transferred from the containment vessel to the air and the air dissipates the transferred heat finally to the plant environment.

While the radiation heat transfer mode is not involved in the decay heat removal systems of water cooled reactors, the mode plays an important role in PSDRS and becomes an unique feature. An understanding of the performance characteristics is required for design of PSDRS. The concept of PSDRS is found in RACS of

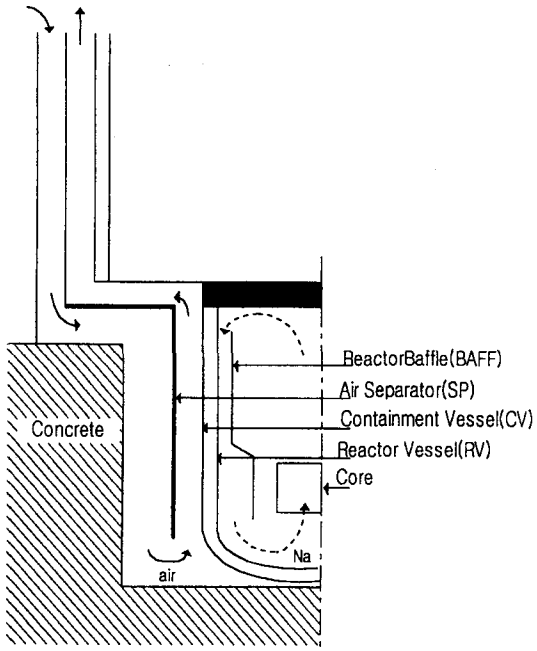

Fig. 1. Structure of the KALIMER PSDRS.

Rockwell International, SAFR[3] and RVACS of GE PRISM[4] but its performance characteristics are not well known in the open literature. This study is a continuation of the work of Reference 5, where the study was limited to the air channel behavior. This study extends the investigation to the air stacks and reactor pool and improves the analysis code algorithm. Based on the investigation results, guidelines for designing PSDRS are set up and the relations between design parameters and performance are analyzed.

2. Development of PARS2

2.1. Heat Transfer Path in PSDRS

As explained in the previous section, the core decay heat is transported to the air flowing in the air channel formed by the containment vessel and air separator. The heat transfer path consists of a

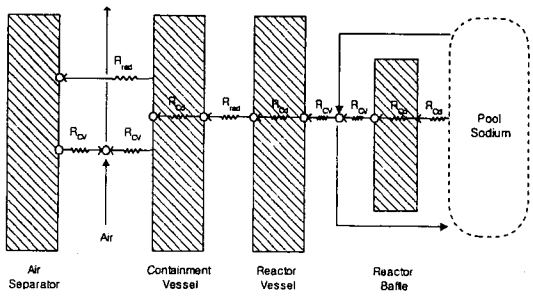

Fig. 2. Heat Transfer Path in the PSDRS.

serial and parallel combination of the heat transfer elements as shown in Fig.2, where R denotes the heat transfer resistance of each element process. In the sodium region, the heat is mainly transported by the sodium convection process of the closed circuit consisting of the core, hot pool, cold pool and annular channel between the reactor baffle and the reactor vessel. There is also an additional path for conduction through the reactor baffle plate. In the air region, the heat from the containment wall is transported to the air in two paths. One is the direct convection path and the other is the indirect path where heat is first transported to the air separator by radiation and then transported to the air by convection from the air separator.

2.2. Mathematical Model

The convection process in the air and sodium flows of Fig. 1 is simulated by the following equations.

$$\frac{\partial \dot{m}}{\partial t}\sum_i \frac{\Delta S_i}{A_i} = \oint \rho g ds - \frac{\dot{m}^2}{2}\sum_i \frac{1}{\bar{\rho}_i A_i^2}\left(K_i + f_i \frac{\Delta S_i}{d_i}\right) \quad (1)$$

$$\frac{\partial}{\partial t}\left(A\Delta x \rho C_p T\right)_{Na,i} = \dot{m}_{Na}\bar{C}_{p,Na}\left(T_{in} - T_{ex}\right)_{Na} + \left(Q_{BAFF} - Q_{RV}\right) + Q_{cond,st} \quad (2)$$

$$\frac{\partial}{\partial t}\left(A\Delta x \rho C_p T\right)_{air,i} = \dot{m}_{air}\bar{C}_p\left(T_{in} - T_{ex}\right)_{air} + Q_{cv} \quad (3)$$

The first equation is a common form for the flow in the sodium flow circuit and that in the air channel. Eqs. (2) and (3) are for the energy balance at a node in the numerical calculation node configuration. They are for the pool sodium channel and for the air channel, respectively. Q_{baff}, Q_{RV}, $Q_{cond,st}$ and Q_{ce} signify the conduction energy flow rates to one cell. They respectively designate heat conducted through the reactor baffle, heat conducted through the reactor vessel wall, heat conducted through sodium in the streamline direction, and heat conducted through the containment vessel wall. Q_{ce} is the sum of the convection from the containment wall and that from the separator which is the same as the heat transfer rate by radiation from the containment wall to the air separator Q^{rad}_{cesp} as shown in Eq. (4).

$$Q_{ce} = hA_{ce}(T_{ce} - T_a) + Q^{rad}_{cesp} \quad (4)$$

Subscripts a, ce and sp signify air, external surface of the containment vessel and internal surface of the air separator, respectively. The heat transfer coefficient is calculated from the Dittus-Boelters correlation[6] and the Skupinshi correlation[6] respectively for the air flow and sodium flow. The Skupinshi correlation reads as Eq. (5).

$$Nu = 4.82 + .0185Pe^{0.827} \quad (5)$$

The conversion of the governing equations into difference equations is made using the boundary node method [7] where a node is located at the boundary in a computation cell. Compared to the conventional scheme where a node is located at the center, the method has the advantage of avoiding the numerical diffusion error and ambiguity in the geometric meaning of a variable value. The ambiguity in the geometric meaning results from the use of the upwind scheme or a similar scheme required for numerical stability in the conventional method.

The expression for radiation heat transfer among several radiation surfaces is written out as Eq.(6)[8].

$$\frac{Q_k}{A_k}\left(\frac{1}{\varepsilon_k} - F_{kk}\frac{1-\varepsilon_k}{\varepsilon_k}\right) - \sum_{j=1,j\neq k}^{n} F_{kj}\frac{Q_j}{A_j}\frac{1-\varepsilon_j}{\varepsilon_j} = -(1-F_{kk})\sigma T_k^4 + \sum_{j=1,j\neq k}^{n} F_{kj}\sigma T_j^4 \quad (6)$$

where F_{kj} is the view factor from surface k to surface j. ε and σ are the emissivity and Stefan-Boltzmann constant, respectively. Though $F_{kk}=0$ in the PSDRS geometry, the equation is still complicated because of the terms representing the radiation interaction between the surfaces at different axial positions, that is, different elevations. When the interaction terms can be neglected, the equation becomes pretty much simplified.

A test was made to check the validity of the neglecting the terms. The view factor was calculated by the Hottel's crossed-string method [8] for the channel consisting of parallel plates located vertically. The test channel represents the geometry of the air channel and configuration of the gap space between the reactor vessel and containment in PSDRS. The vertical length and gap size were taken from the typical PSDRS geometry condition as 16m and 0.2m, respectively. The view factors were calculated for the radiation from the node (originating node) located at the vertical center of the channel to the nodes in the opposite plate (receiving nodes). The distribution of the view factor is shown in Fig. 3 for various configurations of the number of the wall nodes. The view factor to the receiving node, located at the same vertical position as that of the originating node, is the most prominent among the view factors. The values of the most

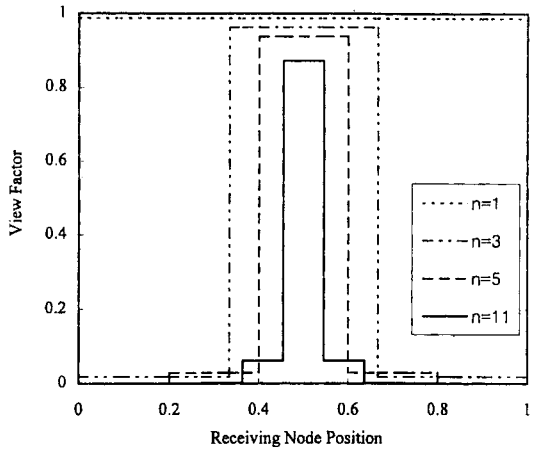

Fig. 3. Distribution of the View Factors(G=0.2m, L=16m).

prominent view factor are 0.99, 0.96, 0.94, and 0.87 when n (=the number of nodes) is 1, 3, 5, and 11, respectively. The reason for the value not being 1.00 for n=1 is that some of the radiation rays from the channel wall escape to the chimney wall at the channel top and to the bottom structure. The view factor value becomes practically zero when the receiving node is located one node away from the center. It shows there is a high possibility that neglect of the radiation interaction terms in Eq. (6) can be made without significant error. The overall effect of the neglect was checked by comparing the calculation results with the terms and those without the terms for the same simple geometry consisting only of the air side. In the checking process, the containment vessel wall temperature was fixed with the linear profile of 520°C at the top and 400°C at the bottom. As shown in Table 1, the difference turned out to be about 1% in the PSDRS heat removal for various conditions of the surface emissivity and node configuration. Based on this observation, the interaction terms are dropped and the equation for the PSDRS radiation heat transfer

Table 1. Effects of the Radiation Interaction Terms

Conditions			Calculation Results	
Emissivity	n	Radiation Interaction Terms	Q[MW]	Air flow rate [Kg/s]
1	10	Yes	3.111	19.745
1	10	No	3.081	19.697
1	3	Yes	3.108	19.699
1	3	No	3.077	19.651
0.8	10	Yes	3.004	19.573
0.8	10	No	2.977	19.530
0.5	10	Yes	2.733	19.113
0.5	10	No	2.714	19.078
0.5	3	Yes	2.731	19.080
0.5	3	No	2.711	19.040

becomes Eq. (7).

$$Q^{rad} = \frac{\sigma A_1 (T_1^4 - T_2^4)}{\frac{1}{\varepsilon_1} + \left(\frac{A_1}{A_2}\right)\left(\frac{1}{\varepsilon_2} - 1\right)} \tag{7}$$

Also the term Q^{rad}_{cesp} in Eq. (4) is expressed using Eq. (7).

The radiation equation, Eq. (7), is highly nonlinear for the unknown variable of the temperature and iteration is required. Several schemes were tested for the iteration and the Newton-Rapshon method was selected. A computer program PARS2 was written to analyze the PSDRS characteristics using the model equations and schemes explained above.

3. Analysis Results

A reference condition was selected from the KALIMER PSDRS design[2] and PARS2 was applied to analyzing the performance characteristics of PSDRS.

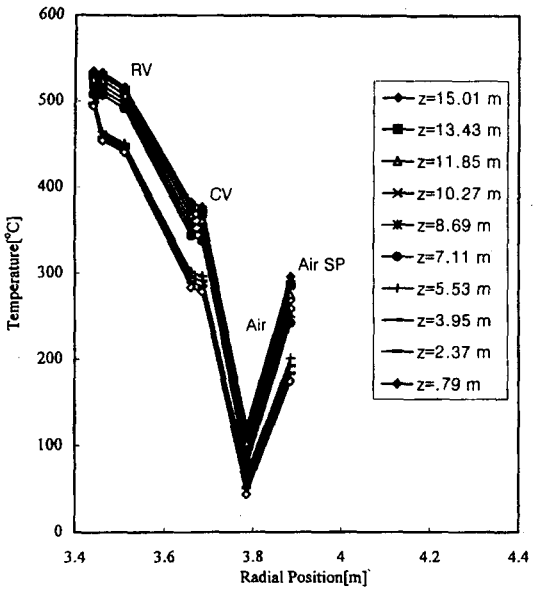

Fig. 4. Temperature Distribution at the Steady State of Q_{decay}=2.5MW.

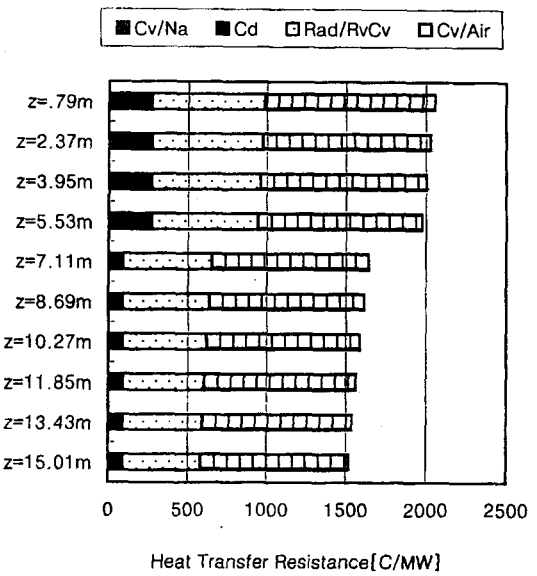

Fig. 5. Distribution of the Heat Transfer Resistances.

3.1. Temperature Distribution and Heat Transfer Resistances

Figs. 4 and 5 are the results for the steady state case where the core decay heat and the channel inlet air temperature are fixed at 2.5 MW and 40°C, respectively. They show the basic characteristics of PSDRS. Fig.4 is for the temperature distribution from the sodium in the annular channel to the air separator with regard to the vertical position. The channel bottom is located at z=0 and the channel top is at z=15.8m. Fig. 5 is for the configuration of the heat transfer resistances that are defined as Eq. (8)

$$R_i = \frac{\Delta T_i}{Q_i} \qquad (8)$$

In Fig. 5, there is the convection resistance between the sodium in the annular channel and internal surface of the reactor vessel R^{conv}_{Na} for the region $z > 5.53$m while the resistance does not appear in the remaining region. This is because the annular channel flow area at the lower region is much larger than that at the upper region as shown in Fig.1 and the flow velocity becomes very different in the two regions. Such difference is also observed in Fig.4 between the two regions. From the figures it is found that the region of the largest resistance is the air region and the resistance in this region accounts for about half of the total and the next region is that of radiation transport between the reactor vessel and containment vessel. As explained previously, there are two modes of heat transfer in the air region. The contribution of the coupled transfer mode of radiation and convection is so significant that the resistance in this region is calculated to reduce to nearly half, by coupling the radiation mode to the convection mode. At the comparison conditions with and without the coupled mode, the difference turned out to be 28% in the

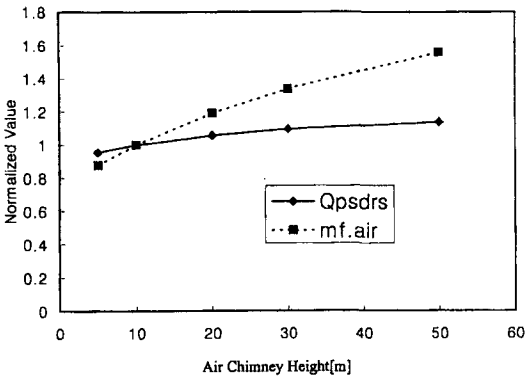

Fig. 6. Effects of the Air Chimney Height on PSDRS Heat Removal Capability and Air Flow Rate.

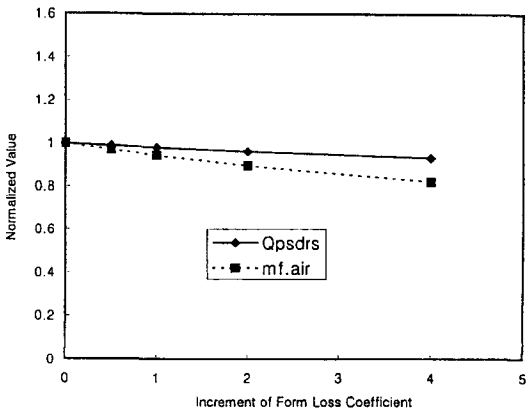

Fig. 7. Effects of the Form Loss Coefficient in the Air Path.

PSDRS heat removal capability. This means that the radiation heat transfer process is very important in PSDRS. The total resistance becomes smaller at a higher position since the temperature becomes higher. Higher temperature makes the radiation transfer process more efficient and also the convection heat transfer coefficient increases by the change of the air property.

3.2. Air Chimney Effects

Figs. 6 and 7 are for the effects of the air chimney design parameter. In the figures, the calculated parameter values were normalized to the values at the reference condition described in Item 3. The effects were calculated by fixing the sodium temperature at 535.83℃ for the top and 491.54℃ for the bottom of the annular sodium channel. The sodium temperatures were taken from one of the typical steady state conditions with the core decay heat = 2.5MW. As expected, the air flow rate mfair and the PSDRS heat removal capacity Q_{psdrs} increase as the chimney height increases since the increase of the natural circulation head is more influential than the friction increase by the chimney length increase. The increase of Q_{psdrs} is, however, only about 15% even though the chimney height is increased from 5m to 50m while mfair is substantially increased. The air convection coefficient increases substantially from the air flow rate increase and the convection resistance decreases considerably. The radiation resistance in the air channel remains nearly unchanged and also there is another major resistance of the radiation between the reactor vessel and containment vessel. Because of these resistance features, Q_{psdrs} marginally changes at the substantial change of the chimney height. This indicates that PSDRS design can be processed by concentrating primarily on the NSSS side parameters and then the BOP (Balance of Plant) parameters such as stack configuration can be treated later as secondary parameters as along as the chimney configuration does not deviate significantly from the reference design configuration.

Fig. 7 shows the effects of the flow resistance change in the air channel. Since the heat transfer resistance in this region is identified as the largest one, improvement of heat transfer in this region can yield the most significant effects in the overall

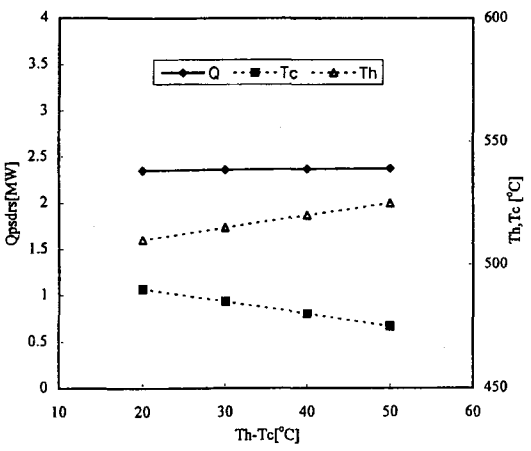

Fig. 8. Effects of the Sodium Temperature Distribution in the Reactor Vessel Channel.

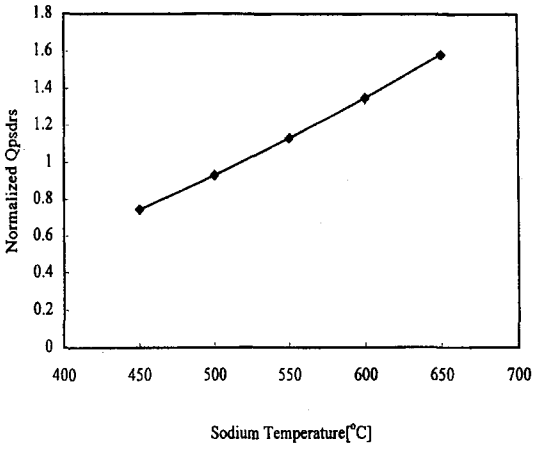

Fig. 9. Effects of the Average Sodium Temperature on the PSDRS Heat Removal Capability.

heat transfer capacity. The improvement requires modification of the air channel wall surface or the addition of a new device and the modification will certainly cause flow resistance increase. The flow resistance increase in turn causes increase in the heat transfer resistance. The sensitivity of Q_{psdrs} upon the change of flow resistance becomes important in getting the improvement. When the form loss coefficient of the pressure head is increased by a magnitude of 4 (equivalent to an 120% increase), the reduction of Q_{psdrs} is only 7%. From this, it is deduced that the situation is promising for increasing the heat removal capability and there is a substantial possibility of enhancing the capability of PSDRS by improving the air channel design.

3.3. Sodium Temperature Effects

Fig. 8 shows the effects of the sodium temperature distribution at the annular channel. The distribution was linear with the highest and lowest temperatures (Th and Tc in the figure) as shown in the figure and the average temperature was kept constant. It shows the temperature distribution effect is negligible on Q_{psdrs} in the checked range as long as the average temperature is the same. This feature simplifies the PSDRS design process pretty much. A designer may consider only the average temperature in handling the PSDRS capacity while neglecting the temperature deviation from the average temperature. The effects of the average sodium temperature on Q_{psdrs} with a uniform temperature profile is shown in Fig. 9, where the calculated Q_{psdrs} was normalized to the Q_{psdrs} at the reference condition. Q_{psdrs} is found to change nearly linearly as the sodium temperature changes with a slightly higher change at a high temperature.

3.4. Reactor Vessel Geometry and Wall Surface Effects

The aspect ratio of a reactor vessel(RV) is closely related to the configuration and sizing of

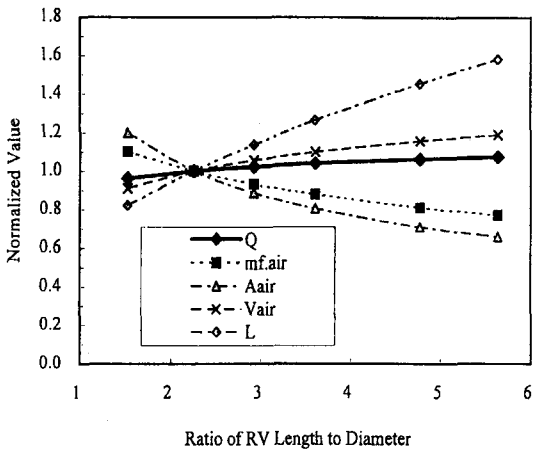

Fig. 10. Effects of the Reactor Vessel Aspect Ratio on the PSDRS Performance.

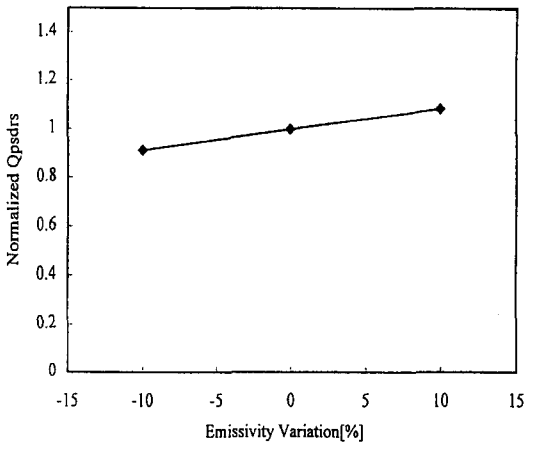

Fig. 11. Effects of the Wall Surface Emissivity.

the equipment placed in the reactor pool and the aspect ratio effect of PSDRS is important not only to the PSDRS design but also to the equipment design and configuration. The aspect ratio effects were studied by changing the aspect ratio L/D(=Length/Outer Diameter of RV). The RV surface area and gaps for RV-CV and CV-SP were kept constant. The RV inner wall temperature was fixed to the linear profile with T_{top} = 520℃ and T_{bottom}=500℃ and the vertical length of the air chimney was set at 10m. Fig. 10 shows the effects on the air flow rate, air flow area size, air velocity and Q_{psdrs}. L and D are respectively 15.8m and 7.02m at the reference condition. As the L/D increases, the air velocity also increases as does the natural circulation head but the channel air flow rate decreases. The trend comes from that the effects of the increase in the air velocity are smaller than the effects of the decrease in the air flow area. For the PSDRS heat removal capacity, there are competing effects upon the increase of L/D. The positive effect is the increase of the convection heat transfer coefficient by the velocity increase and the air channel heat transfer area increase. Though the reactor vessel surface area is kept constant, the containment vessel and air separator surface areas are increased since the gaps between the vessels are kept constant and the radii of the containment vessel and air separator are larger than the reactor vessel radius. The negative effect comes from the flow rate decrease. The decrease causes an increase in the air temperature. This increase reduces the temperature difference between the air and vessel wall, which is the driving force of the heat transfer. From the competing effects, the sensitivity of the PSDRS capacity upon the L/D change becomes very small as shown in Fig. 10. At the 60% increase of L/D, Q_{psdrs} increases only 4%.

Fig. 11 shows the effect of the surface emissivity. The emissivity for the RV, CV, and SP was changed from the reference value of 0.77, 0.85, and 0.85 by the same ratio of 10%. The sensitivity is found to be nearly 1 with 9% change in Q_{psdrs} at the 10% emissivity change.

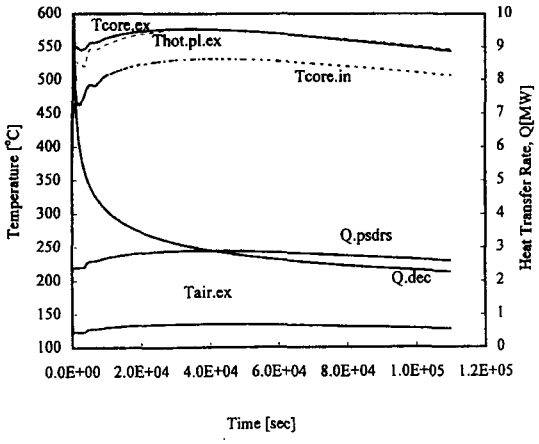

Fig. 12. Transient Behavior of PSDRS Parameters.

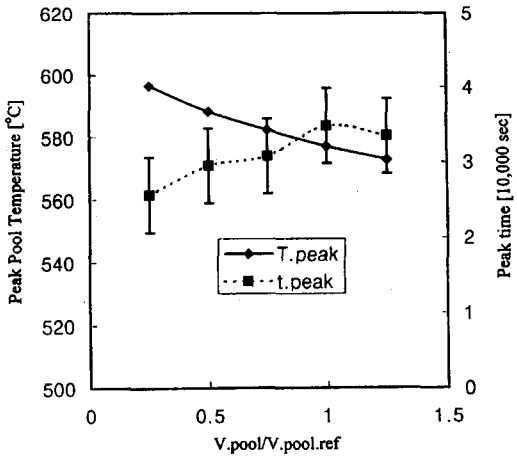

Fig. 13. Effects of the Reactor Pool Volume on the Peak Time and Temperature.

3.5. Transient Effects

Fig. 12 shows the transient calculation results. At the initial stage, the core decay heat rate is larger than the PSDRS heat removal capability and the sodium temperature increases. The increase of the sodium temperature also increases the PSDRS capability. Also the core decay heat decreases as time elapses and the sodium temperature reaches its peak at the time when the heat removal rate by PSDRS matches the core decay heat rate.

Fig. 13 shows the effects of the reactor pool volume size on the peak temperature T_{peak} and the peak time t_{peak} that is the time when the sodium reaches its peak temperature. The uncertainty range of the peak time indicated in the figure is relatively large since the time step is internally adjusted in PARS2 and the time step becomes very large when the sodium reaches its peak temperature. The peak temperature decreases, as expected, and the peak temperature is reached at a later time when the sodium pool volume increases. Quantitatively speaking, the peak temperature is changed by about 6°C at the 30% change of the pool volume.

4. Conclusions

PARS2, a thermal performance analysis code for PSDRS, was developed and applied to the analysis of the relation between PSDRS design parameters and performance. The major findings are summarized below.

1) The radiation heat transfer in PSDRS can be modeled without significant error neglecting the terms accounting for the radiation interaction between the nodes at different altitudes.
2) The heat transfer mechanism
   - The largest heat transfer resistance in PSDRS is at the air channel region.
   - There is a substantial possibility of enhancing the performance of PSDRS by improving the air channel design.
2) The major design parameters were found to be

the parameters from the reactor vessel to the air separator, and PSDRS design can be practically made decoupling the air chimney parameters at the initial stage.

Acknowledgement

This work was performed under the Long-and-Mid-term Nuclear R&D Program sponsored by the Ministry of Science and Technology of Korea.

Nomenclature

A	area
$\overline{C_p}$	average of the specific heat at constant pressure
CV	containment vessel
F	view factor
f	friction coefficient
g	gravitational acceleration
h	convection heat transfer coefficient
K	form loss coefficient in pressure drop
$\dot{m}$	mass flow rate
n	number of nodes
Nu	Nusselt number
Pe	Peclet number
Q	heat transfer rate
R	heat transfer resitance
RV	reactor vessel
S	stream line
SP	air separator
T	temperature

Greek letters

ϵ	emissivity
$\overline{\rho}$	density
σ	Stefan-Boltzmann constant

Superscripts

conv	convection heat transfer
rad	radiation heat transfer

Subscripts

a	air
BAFF	reactor baffle
ce	external surface of containment vessel
cd,cond	conduction heat transfer
cv	convection heat transfer
ex	exit
i	node index, dummy variable
in	inlet
n	number of radiation structures
rad	radiation heat transfer
RV	reactor vessel
sp	air separator
t	total

References

1. Park C.K. et al, KALIMER Design Concept Report, KAERI Report, KAERI/TR-888/97, KAERI, July (1997).
2. Wi Myung Hwan, System Description for RHRS, KALIMER/FS500-DD-01/1998, KAERI, (1998).
3. Lancet R.T., Marchaterre J.F., Inherent Safety of the SAFR Plant, Proceedings of the International Topical Meeting on Fast Reactor Safety, CONF-850410, pp.653-659, Knoxville, TN, USA, May (1985).
4. GE, PSID-Preliminary Safety Information Document, GEFR-00793/UC-87 Ta, GE, USA, December (1987).
5. SimY.S., Wi M.H., Kim Y.S., KimY.C., Cho M, "Elevation Configuration of KALIMER Intermediate System",IAEA-TECDOC-907, pp.213-224, Vienna, IAEA, (1996).
6. Holman J.P., Heat Transfer, 6th ed., p.274, p.307, McGraw-Hill Book Company, New York, USA, (1986).

7. Sim Y.S., Kim Y.S. "Analysis Characteristics of the Cross flow Heat Transfer in a Soium Shell-and-tube Heat Exchanger", Proceeding of the Korean Nuclear Society, May(1996).

8. Siegel R., Howell J.R., Thermal Radiation Heat Transfer, 2nd ed.,p.243,p.203, Hemisphere Pub. Co., Washington, USA, (1981).